Dalton Transactions

Accepted Manuscript

Volume 1 | Number 1 | Jan 2013 | Pages 1–100
Dalton Transactions
An international journal of inorganic chemistry
www.rsc.org/dalton
ROYAL SOCIETY OF CHEMISTRY

This is an *Accepted Manuscript*, which has been through the Royal Society of Chemistry peer review process and has been accepted for publication.

Accepted Manuscripts are published online shortly after acceptance, before technical editing, formatting and proof reading. Using this free service, authors can make their results available to the community, in citable form, before we publish the edited article. We will replace this *Accepted Manuscript* with the edited and formatted *Advance Article* as soon as it is available.

You can find more information about *Accepted Manuscripts* in the Information for Authors.

Please note that technical editing may introduce minor changes to the text and/or graphics, which may alter content. The journal's standard Terms & Conditions and the Ethical guidelines still apply. In no event shall the Royal Society of Chemistry be held responsible for any errors or omissions in this *Accepted Manuscript* or any consequences arising from the use of any information it contains.

ROYAL SOCIETY OF CHEMISTRY

www.rsc.org/dalton

Dalton Transactions

Paper

μ_3-Oxo stabilized by three metal cations is a sufficient nucleophile for enzymatic hydrolysis of phosphate monoesters

Received 00th January 20xx,

Accepted 00th January 20xx

DOI: 10.1039/x0xx00000x

www.rsc.org/

Jian-Nan Ji and Shi-Lu Chen*

Diverse species have previously been proposed to be effective nucleophiles in enzymatic hydrolysis of phosphate esters. A novel penta-metal cluster (two Fe^{3+} and three Ca^{2+}) was recently discovered in the active site of PhoX alkaline phosphatase, with the revelation of an architecture of μ_3-oxo bridging one Ca^{2+} and two antiferromagnetically coupled Fe^{3+}. In this work, using density functional theory calculations, the μ_3-oxo stabilized by three cations has been demonstrated to be a new type of effective nucleophile. The calculations give a strong support to the "ping-pong" mechanism involving the nucleophilic attack of the μ_3-oxo on the substrate phosphor and the subsequent hydrolysis of the covalent phospho-enzyme intermediate. A base mechanism with the μ_3-oxo acting as a general base to activate an additional water has further been demonstrated to be inaccessible. The results advance the understanding of enzymatic hydrolysis of phosphate esters and may give important inspiration for the exploration of multinuclear biomimetic catalysts.

1 Introduction

Enzymatic hydrolysis of phosphate esters play significant roles in various biological processes such as biological detoxification, energy and signal transduction, the replication of the genetic material, etc.[1-8] In such reactions, the nucleophile mechanism initiated by a nucleophilic attack on the substrate phosphor is widely employed.[9-13] Diverse species have been proposed to be effective nucleophiles (Fig. 1), including the cysteine thiolate (protein tyrosine phosphatases),[14-18] the serine alkoxide (PhoA alkaline phosphatases),[19-22] the terminal hydroxide coordinating to one metal ion (a few purple acid phosphatases[23,24] and 3'-5' exonucleases[25,26]), and especially the bridging hydroxide stabilized by two metal cations (phosphotriesterase,[27-29] Ser/Thr protein phosphatases,[30-32] phospholipase C,[33] nuclease P1,[34] RNase Z,[35] etc). Quite recently, a novel penta-metal cluster (two Fe^{3+} and three Ca^{2+}) was discovered in the active site of PhoX alkaline phosphatase from *Pseudomonas fluorescens* (Fig. 2.A), with the revelation of an architecture of μ_3-oxo bridging three of the metals (one Ca^{2+} and two antiferromagnetically coupled Fe^{3+}). PhoX catalyzes the hydrolysis of phosphate monoesters ranging from alkyl to aryl phosphates (Fig. 2.B).[12] The PhoX reaction mechanism turns out to be very attractive for the understanding of the chemistry of phosphate ester hydrolysis. Does PhoX also employ the nucleophile mechanism? In particular, can the μ_3-oxo stabilized by three cations serve as a new type of nucleophile in the hydrolysis of phosphate esters? The scrutiny into this is of significance for the interpretation of this new piece in phosphate ester hydrolysis and may give useful inspiration to the exploration of multinuclear biomimetic catalysts.

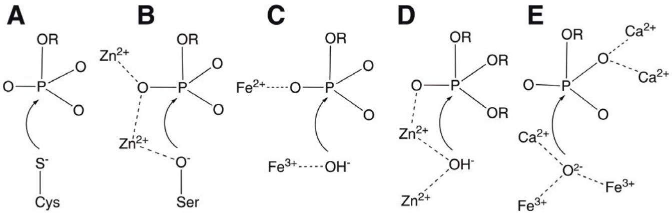

Fig. 1 Diverse nucleophiles in enzymatic hydrolysis of phosphate esters, including cysteine thiolate (A), serine alkoxide (B), terminal hydroxide (C), μ_2-bridging hydroxide (D), and μ_3-bridging oxo (E).

In the present work, using unrestricted density functional theory (UDFT) with the hybrid functional B3LYP,[36-38] we have investigated the reaction mechanism of PhoX alkaline phosphatase. Two substrates were considered, i.e., methyl and p-nitrophenyl phosphates, which represent alkyl and aryl phosphates, respectively. We here present the energetics for the PhoX-catalyzed hydrolysis of methyl and p-nitrophenyl phosphates and provide the characterization of the stationary points involved. It has been demonstrated that the nucleophilicity of the μ_3-oxo stabilized by three cations is sufficient to be utilized in the hydrolysis of phosphate monoesters.

Key Laboratory of Cluster Science of Ministry of Education, Beijing Key Laboratory of Photoelectronic/Electrophotonic Conversion Materials, School of Chemistry, Beijing Institute of Technology, Beijing 100081, China. E-mail: shlchen@bit.edu.cn

Electronic Supplementary Information (ESI) available: Supplementary table, figures, and schemes, and Cartesian coordinates and absolute energies of all optimized structures. See DOI: 10.1039/x0xx00000x

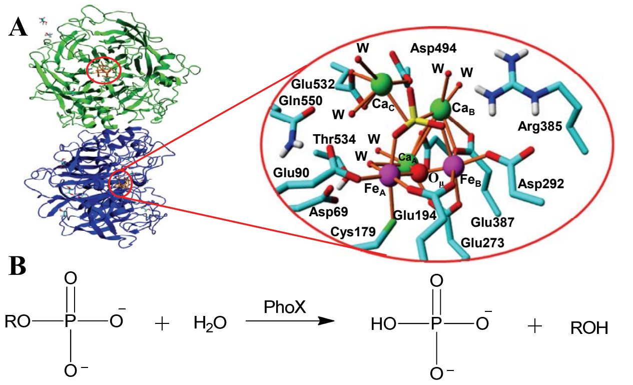

Fig. 2 Overall view of the PhoX structure and close-up view of the active site with a Pi bound (A), and hydrolysis of phosphate monoesters catalyzed by PhoX alkaline phosphatase (B). Coordinates from PDB entry 4ALF were used to generate the pictures in A. The water molecules are referred to as W. The μ_3-oxo is indicated by O_μ. Schematic ligand interactions in the PhoX active site are given in Fig. S1 in the Electronic Supplementary Information (ESI).

2 Computational methods

All calculations were performed using unrestricted density functional theory (UDFT) with the hybrid functional B3LYP[36-38] as implemented in the Jaguar 7.6 package.[39] Geometry optimizations were carried out with the lacvp basis set[40] for the Fe and Ca atoms, the 6-311+G(d) for P, the 6-31G(d,p) for waters, the functional groups of residues, and the substrate atoms except for P, and the 6-31G for the alkyl chains of residues. Based on the optimized geometries, more accurate energies were obtained by performing single point calculations with larger basis sets, i.e. lacv3p+ for Fe and Ca and cc-pvtz(-f) for other elements. To estimate the effects of the protein environment on the calculated energies, solvation effects were calculated at the same theory level as the optimizations by performing single point calculations on the optimized structures using the self-consistent reaction field method with a Poisson-Boltzmann solver[41,42] and a dielectric constant (ε) of 4 which is a standard value that has been used in many previous studies.[43-45] Using Gaussian 03,[46] frequency calculations were performed at the same theory level as the optimizations to obtain zero-point energies (ZPE) and to confirm the nature of the stationary points. As mentioned later, some atoms were kept fixed to their X-ray crystal positions. An investigation of varying constraints with acetylene hydratase[47] as an example indicates that the coordinate error has very small effect on the calculated energies when the resolution of the starting crystal structure is better than 2.0 Å (1.25 Å in the present case).[12] Another study of phosphotriesterase[48] also shows that the energy differences between with and without atom fixation are not of such a magnitude that they will alter any conclusion about the mechanism. Dispersion corrections were calculated using the empirical formula by Grimme et al. (i.e., DFT-D3).[49-52] The energies reported here have been corrected for solvation, zero-point vibrational, and dispersion effects. The present procedure has been well benchmarked[43,45,48,53,54] and successfully used to study a large number of enzyme mechanisms in the past decade. A comprehensive review has been written recently.[43]

3 Results and discussion

The X-ray crystal structure of PhoX (PDB code: 4ALF)[12] was used to build a model of the PhoX active site (see Fig. 3). The chemical model contains the five metal ions (two Fe^{3+} and three Ca^{2+}), the bridging μ_3-oxo (O_μ), the first-shell ligands (Glu90, Glu194, Glu273, Glu387, Glu532, Asp292, Asp479, Asp494, Cys179, and six water molecules), and four second-shell residues (Asp69, Thr534, Arg385 and Gln550) which are hydrogen bonding to the first-shell ligands. To reduce the size, some truncations were made so that in principle the side chains of residues were kept. To preserve the spatial arrangement of the residues, the atoms where the truncations have been done were kept frozen to their X-ray crystal positions. This procedure has been indicated by careful benchmarks to have little effect on the calculated energies.[47,48] The total charge of the model is -1 and the total number of atoms without substrates included is 186.

With methyl phosphate included, the present model of the PhoX active site was optimized at diverse electronic states (see Table S1 in the ESI). The ground state of enzyme-substrate complex (referred to as $\mathbf{React_{me}}$) was found to be at the singlet state with the two high-spin iron cations antiferromagnetically coupled (Table S1), consistent with the experimental finding.[12] In $\mathbf{React_{me}}$, the unpaired spins at Fe_A and Fe_B are computed to be 3.94 and -4.09, respectively, with a little delocalization at the O_μ atom (-0.21). The substrate is tightly bound by the metal cluster (see Figs. 3 and 4). It is shown that two phosphoryl oxygens respectively coordinate to Fe_A and Fe_B (the two O-Fe distances are 2.22 and 2.16 Å, respectively) and the third phosphoryl oxygen binds to Ca_B and Ca_C. The ester oxygen (denoted by O_{lg}) is hydrogen bonding to a water bound by Ca_C (named by W_C). With this, the phosphor center is located at a distance of 2.82 Å to O_μ, a reasonable distance for the initial step of nucleophilic attack.

Dalton Transactions

Paper

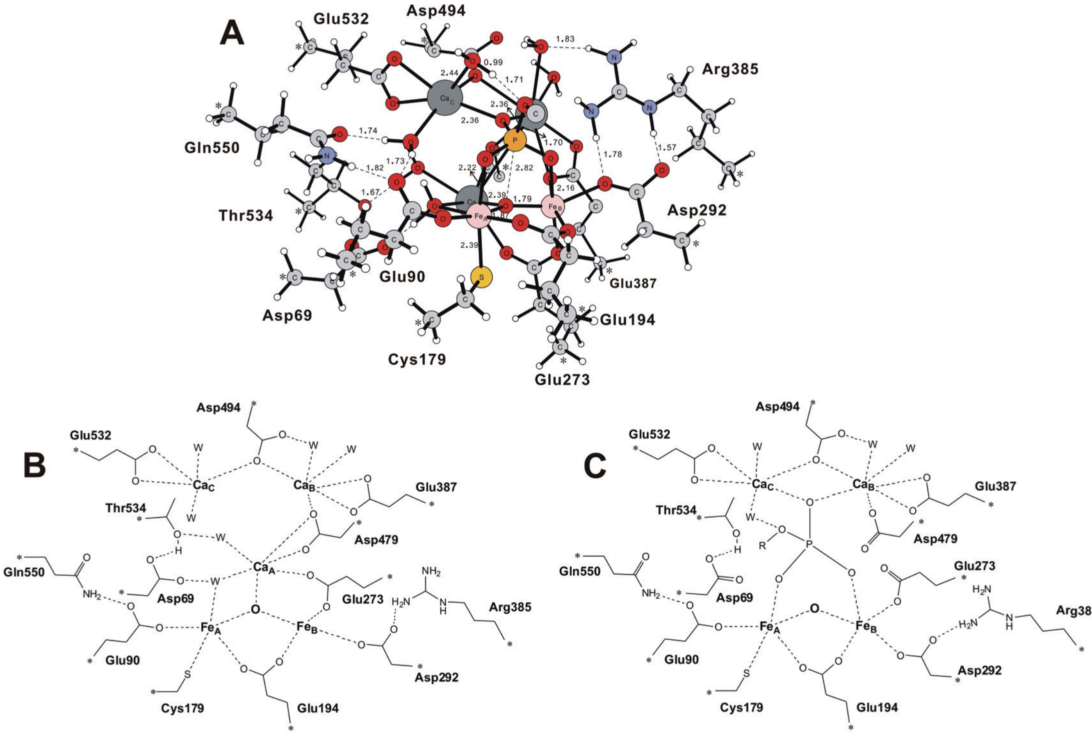

PhoX active site without substrate shown

PhoX active site with substrate shown

Fig. 3 Optimized structure of the PhoX active site with a methyl phosphate bound (A) and its schematic structures without (B) and with (C) substrate shown. For clarity, some atoms are omitted (e.g. the Ca_A in C). Asterisks indicate the atoms which are fixed to their X-ray positions. Water molecules are denoted by W. All distances are in angstrom (Å).

From **React$_{me}$**, a transition state (**TS$_{me}$**, Fig. 4) for the nucleophilic attack of O_μ on the substrate phosphor has been optimized and confirmed to be a first-order saddle point with an imaginary frequency of 116*i* cm^{-1}. This step turns out to be a S_N2-type concerted displacement, i.e., simultaneously with the O_μ-P bond formed, the P-O_{lg} ester bond is broken. It can thus be called by phosphoryl transfer. In **TS$_{me}$**, the key distances of the phosphor to the O_μ and the leaving group oxygen (O_{lg}) are 1.96 and 1.88 Å, respectively. The phosphoryl transfer results in a covalent phospho-enzyme intermediate (**Int$_{me}$**, Fig. 4), with a O_μ-P bond distance of 1.64 Å. It is interesting to find that the leaving methoxide is immediately protonated by the Ca_C-activated W_C water, leading to a Ca_C-stabilized hydroxide (O_CH^-) and a free methanol product hydrogen-bonding to the former. The former most likely acts as another nucleophile in the next step of the hydrolysis of the phospho-enzyme intermediate. Furthermore, the More-O'Ferral-Jencks (MFJ) plot (Fig. 4),[55,56] which defines the reaction pathway in terms of the O_μ-P and P-O_{lg} distances, indicates that the nature of phosphoryl transfer is concerted associative.

With solvation effects of the surrounding protein and dispersion effects added, the phosphoryl transfer is calculated to have a barrier of 11.8 kcal/mol (Fig. 5.A). This clearly demonstrates that this step is energetically accessible and the μ_3-oxo stabilized by three metal cations is nucleophilic enough to be utilized in the phosphoryl transfer. In this step, the Lewis acidic metal ions may play a role to stabilize the negative charge developing in the nucleophilic attack, thereby lowering the energy barriers. The resultant intermediate (**Int$_{me}$**) lies 7.8 kcal/mol lower than **React$_{me}$**, showing a quite large exothermicity.

We also examined the dissociative mechanism, where the covalent bond between the phosphor center and the O_{lg} oxygen is already broken before the O_μ-P bond is formed, leading to a positive-charge-increased tri-coordinated metaphosphate intermediate (see Scheme S1 in the ESI). However, any attempts to optimize this tri-coordinated metaphosphate intermediate failed and all resulted in the penta-coordinated intermediate described earlier. This may implies that the dissociative mechanism does not exist in PhoX. The same results (associative mechanism instead of dissociative mechanism) have been found in the cases of phosphotriesterase (di-zinc enzyme)[27] and PhoA alkaline phosphatase (tri-metal enzyme).[21] A possible reason for the achievement of associative mechanism in these three enzymes is that the parts directly binding to phosphate moiety are positively charged, including several metal cations. These local cationic surroundings most likely prefer an associative mechanism, in which negative charge is increased during the catalysis.[57]

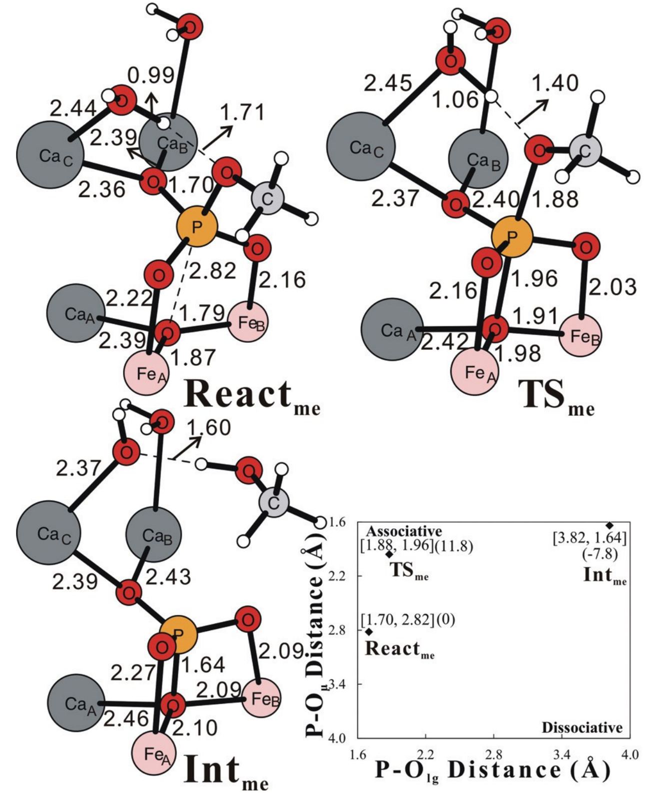
0.99
2.44
2.39
Ca$_C$
Ca$_B$
1.71
2.36
1.70
C
P
2.82
2.16
Ca$_A$
2.22
1.79
Fe$_B$
2.39
1.87
Fe$_A$
React$_{me}$
2.45
1.06
1.40
Ca$_C$
Ca$_B$
2.37
2.40
1.88
P
2.16
1.96
2.03
Ca$_A$
1.91
Fe$_B$
2.42
1.98
Fe$_A$
TS$_{me}$
1.60
2.37
C
Ca$_C$
Ca$_B$
2.39
2.43
P
2.09
2.27
1.64
Ca$_A$
2.09
Fe$_B$
2.46
2.10
Fe$_A$
Int$_{me}$
Associative
[1.88, 1.96](11.8)
TS$_{me}$
[3.82, 1.64]
(-7.8)
Int$_{me}$
[1.70, 2.82](0)
React$_{me}$
Dissociative
P-O$_\mu$ Distance (Å)
1.6
2.2
2.8
3.4
4.0
P-O$_{lg}$ Distance (Å)

Fig. 4 Optimized structures of stationary points for the phosphoryl transfer in the methyl phosphate hydrolysis and the corresponding More–O'Ferral–Jencks (MFJ) plot. For clarity, ligands are omitted except for some key water molecules. All distances are indicated in angstrom (Å). In the MFJ plot, the key distances of the phosphor to the leaving group oxygen (P-O$_{lg}$) and the nucleophile oxygen (P-O$_\mu$) are given in square brackets, and relative energies (kcal/mol) are provided in parentheses.

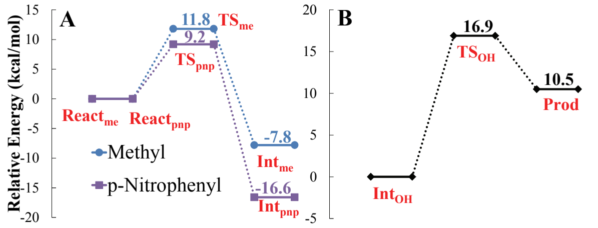

Fig. 5 Potential energy profiles for the phosphoryl transfer (**A**) and the hydrolysis of phospho-enzyme intermediate (B) in the PhoX-catalyzed reactions. Methyl: methyl phosphate. p-Nitrophenyl: p-nitrophenyl phosphate.

When the methanol product was removed from **Int$_{me}$**, the O$_C$H$^-$ lost the hydrogen bond to the methanol and then was immediately protonated by an adjacent water coordinating to Ca$_B$ (see **Int$_{OH}$** in Fig. 6), resulting in a new Ca$_C$-bound water (W$_C$) and a Ca$_B$-stabilized hydroxide (O$_B$H$^-$). In **Int$_{OH}$**, the W$_C$ oxygen (O$_C$) is 3.34 Å away from the phosphor and orientated at a perfect position to attack on the phosphor from the opposite side of O$_\mu$. A transition state of this kind (**TS$_{OH}$**, Fig. 6) has been optimized with the distances of the P to the O$_C$ and O$_\mu$ to be 2.07 and 1.77 Å, respectively. By the frequency analysis and MFJ plot (Fig. 6), the nature of **TS$_{OH}$** has also been confirmed to be a S$_N$2-type concerted associative displacement, that is, the W$_C$ water performs the nucleophilic attack on the P center to replace the μ_3-oxo (meanwhile, one proton of W$_C$ is transferred back to the O$_B$H$^-$). The displacement, also named by the hydrolysis of phospho-enzyme intermediate, leads to a product of inorganic phosphate and a regenerated active site (**Prod**, Fig. 6).

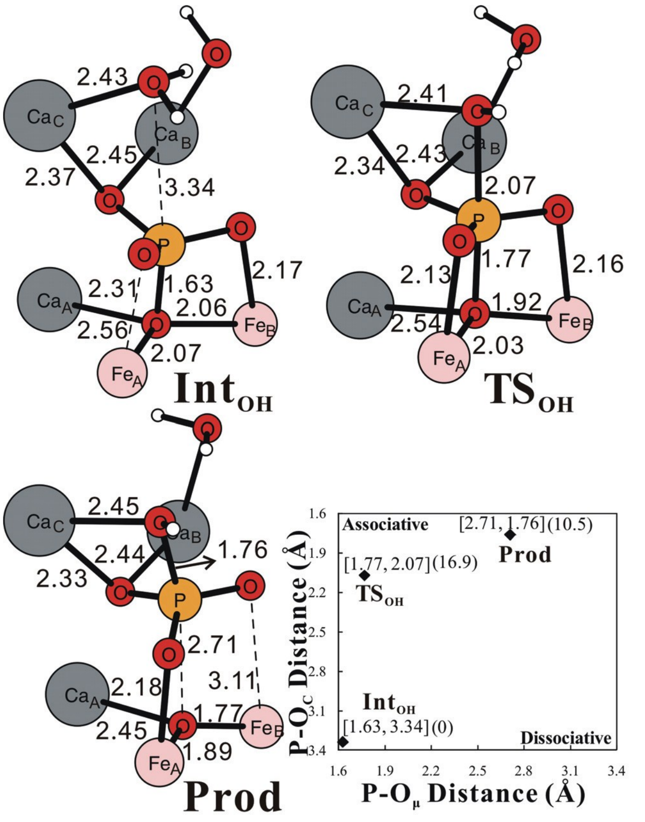
2.43
Ca$_C$
Ca$_B$
2.45
2.37
3.34
P
2.17
Ca$_A$
2.31
1.63
2.06
Fe$_B$
2.56
2.07
Fe$_A$
Int$_{OH}$
2.41
Ca$_C$
Ca$_B$
2.34
2.43
2.07
P
2.13
1.77
2.16
Ca$_A$
1.92
Fe$_B$
2.54
2.03
Fe$_A$
TS$_{OH}$
2.45
Ca$_C$
Ca$_B$
2.44
1.76
2.33
P
2.71
3.11
Ca$_A$
2.18
1.77
Fe$_B$
2.45
1.89
Fe$_A$
Prod
Associative
[2.71, 1.76](10.5)
Prod
[1.77, 2.07](16.9)
TS$_{OH}$
Int$_{OH}$
[1.63, 3.34](0)
Dissociative
P-O$_C$ Distance (Å)
1.6
1.9
2.2
2.5
2.8
3.1
3.4
P-O$_\mu$ Distance (Å)

Fig. 6 Optimized structures of stationary points in the hydrolysis of phospho-enzyme intermediate and the corresponding More–O'Ferral–Jencks (MFJ) plot.

The barrier of this step (16.9 kcal/mol) is predicted to be higher than that of phosphoryl transfer (11.8 kcal/mol) (Fig. 5.B), indicating that the hydrolysis of phospho-enzyme intermediate is rate-limiting in the overall reaction. This result, along with an endothermicity of 10.5 kcal/mol in the second step (Fig. 5.B), probably implies that the μ_3-oxo stabilized by three cations may be a stronger nucleophile than the hydroxide bound by one metal ion. On the other hand, the binding of an oxygen species (probably an original water) to three metal ions may significantly lower its pK_a, thus facilitating the formation and stabilization of a μ_3-oxo species.

The PhoX-catalyzed hydrolysis of p-nitrophenyl phosphate follows the same pattern as the case of methyl phosphate and similar stationary points have been optimized (see Fig. 7). The transition state (**TS$_{pnp}$**) for the step of phosphoryl transfer was also shown to be S$_N$2-type concerted associative. In **TS$_{pnp}$**, the O$_\mu$-P and P-O$_{lg}$ distances are computed to be 2.13 and 1.99 Å, respectively, which are slightly longer than the corresponding distances in **TS$_{me}$** (1.96 and 1.88 Å), indicating that the nature of phosphoryl transfer trends toward the dissociative direction when the pK_a of the leaving group decreases.

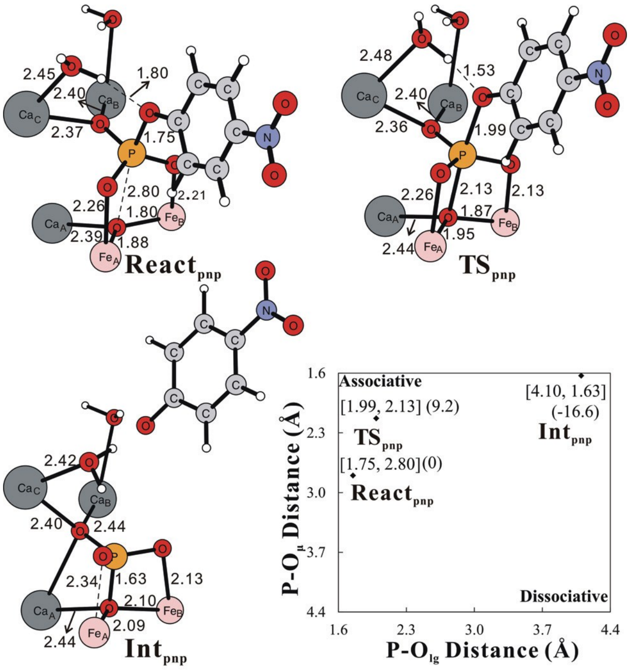

Fig. 7 Optimized structures of stationary points for the phosphoryl transfer in the p-nitrophenyl phosphate hydrolysis and the corresponding More–O'Ferral–Jencks (MFJ) plot.

Since p-nitrophenolate is a better leaving group, it is reasonable to observe that the barrier (9.2 kcal/mol) is 2.6 kcal/mol lower than that in the case of methyl phosphate (Fig. 5.A). The resulting p-nitrophenolate was not protonated by the W$_C$ water due to its low pK_a. To perform the second displacement, the W$_C$ water may be activated by other general base or the hydroxide from solution. For all phosphate monoester substrates, the step of the phospho-enzyme hydrolysis may be identical as the nucleophile (O$_C$H$^-$) and the leaving group (μ_3-oxo) are probably reserved.

In phosphotriesterase (PTE) a base mechanism was also suggested, in which the bridging hydroxide acts as a base (instead of a nucleophile) to abstract a proton from a water molecule leading to another hydroxide and then the resultant hydroxide performs a nucleophilic attack on the substrate phosphor (see Scheme S2).[58] Although this kind of base mechanism has been demonstrated to be unfavorable in PTE by the X-ray crystal structures and DFT calculations,[28] it is still necessary to examine its feasibility in the present case of PhoX. Based on the chemical model of Fig. 3, an additional water molecule (**Wat**) was added to optimize an enzyme-methyl phosphate complex with the **Wat** coordinated to the Fe$_B$ ion (denoted by **React$_{base}$**, Fig. S2 in the ESI). From **React$_{base}$**, a transition state (**TS$_{base}$**, Fig. S2) with the **Wat** oxygen attacking the P has been optimized. In **TS$_{base}$**, the distances of the phosphor to the leaving group oxygen and the added water oxygen (O$_{ad}$) are 2.32 and 1.86 Å, respectively. It has been confirmed by the frequency analysis that simultaneously with the O$_{ad}$-P bond formation, one **Wat** proton is transferred to the μ_3-oxo (O$_\mu$), indicating that the μ_3-oxo serves as a general base to activate the attacking water. This step results in an enzyme-product complex (**Prod$_{base}$**, Fig. S2) which is quite similar to the crystal structure of PhoX with inorganic phosphate bound.[12] For example, the O$_\mu$-P, O$_\mu$-Fe$_A$, O$_\mu$-Fe$_B$, and O$_\mu$-Ca$_A$ distances in **Prod$_{base}$** are 2.93 2.09, 1.98, and 2.46 Å respectively, to be compared to the crystallographic distances of 2.84, 1.98, 1.95, and 2.40 Å respectively. Therefore, the base mechanism in PhoX could not be simply ruled out by the geometrical analysis. However, the energy barrier is calculated to be very high (33.8 kcal/mol), a value that indicates the infeasibility of base mechanism in PhoX.

4 Conclusions

In summary, the calculations present strong evidences to the hypothesized "ping-pong" mechanism in the PhoX-catalyzed hydrolysis of phosphate monoesters,[12] where two S$_N$2-type chemical displacements take place, i.e., the phosphoryl transfer initiated by the nucleophilic attack of the μ_3-oxo on the substrate phosphor and the subsequent hydrolysis of the covalent phospho-enzyme intermediate. In the catalytic cycle, the configuration at the phosphor center is retained and the μ_3-oxo oxygen is always conserved in the active site. In particular, it has been demonstrated that the μ_3-oxo stabilized by three metal cations is a new type of nucleophile whose nucleophilicity is sufficient to be utilized in the hydrolysis reaction, a feature that advances the understanding of this missing piece in enzymatic hydrolysis of phosphate esters and may be inspiring for the exploration of multinuclear biomimetic catalysts. Furthermore, a base mechanism, where the μ_3-oxo acts as a general base (instead of a nucleophile) to activate the nucleophilic water molecule, has been demonstrated to be unreachable in PhoX.

Acknowledgements

This work was financially supported by the National Natural Science Foundation of China (21373027), Beijing Nova Program (Z151100000315055), and the 111 Project (B07012).

References

1 S. J. Benkovic and K. J. Schray, Academic Press, New York, 1973, vol. 8, pp. 201-238.
2 A. S. Mildvan, *Adv. Enzymol.*, 1979, **49**, 103-126.
3 F. H. Westheimer, *Chem. Rev.*, 1981, **81**, 313-326.
4 I. R. Vetter and A. Wittinghofer, *Q. Rev. Biophys.*, 1999, **32**, 1-56.
5 S. C. Kamerlin, P. K. Sharma, R. B. Prasad and A. Warshel, *Q. Rev. Biophys.*, 2013, **46**, 1-132.
6 W. W. Cleland and A. C. Hengge, *Chem. Rev.*, 2006, **106**, 3252-3278.
7 N. Mitic, S. J. Smith, A. Neves, L. W. Guddat, L. R. Gahan and G. Schenk, *Chem. Rev.*, 2006, **106**, 3338-3363.
8 J. Weston, *Chem. Rev.*, 2005, **105**, 2151-2174.
9 D. M. Karl, *Nature*, 2000, **406**, 31-33.
10 L. L. Clark, E. D. Ingall and R. Benner, *Nature*, 1998, **393**, 426-426.

11 S. Kathuria and A. C. Martiny, *Environ. Microbiol.*, 2011, **13**, 74-83.

12 S. C. Yong, P. Roversi, J. Lillington, F. Rodriguez, M. Krehenbrink, O. B. Zeldin, E. F. Garman, S. M. Lea and B. C. Berks, *Science*, 2014, **345**, 1170-1173.

13 J. R. Knowles, *Annu. Rev. Biochem.*, 1980, **49**, 877-919.

14 A. D. Pannifer, A. J. Flint, N. K. Tonks and D. Barford, *J. Biol. Chem.*, 1998, **273**, 10454-10462.

15 H. Cho, R. Krishnaraj, E. Kitas, W. Bannwarth, C. T. Walsh and K. S. Anderson, *J. Am. Chem. Soc.*, 1992, **114**, 7296-7298.

16 J. M. Denu, D. L. Lohse, J. Vijayalakshmi, M. A. Saper and J. E. Dixon, *Proc. Natl. Acad. Sci. U. S. A.*, 1996, **93**, 2493-2498.

17 K. L. Guan and J. E. Dixon, *J. Biol. Chem.*, 1991, **266**, 17026-17030.

18 G. Zhou, J. M. Denu, L. Wu and J. E. Dixon, *J. Biol. Chem.*, 1994, **269**, 28084-28090.

19 V. Lopez-Canut, M. Roca, J. Bertran, V. Moliner and I. Tunon, *J. Am. Chem. Soc.*, 2011, **133**, 12050-12062.

20 G. Hou and Q. Cui, *J. Am. Chem. Soc.*, 2012, **134**, 229-246.

21 S.-L. Chen and R.-Z. Liao, *Chemphyschem*, 2014, **15**, 2321-2330.

22 J. K. Lassila, J. G. Zalatan and D. Herschlag, *Annu. Rev. Biochem.*, 2011, **80**, 669-702.

23 M. B. Twitchett and A. G. Sykes, *Eur. J. Inorg. Chem.*, 1999, **1999**, 2105-2115.

24 M. B. Twitchett, G. Schenk, M. A. Aquino, D. T. Yiu, T. C. Lau and A. G. Sykes, *Inorg. Chem.*, 2002, **41**, 5787-5794.

25 S. Hamdan, P. D. Carr, S. E. Brown, D. L. Ollis and N. E. Dixon, *Structure*, 2002, **10**, 535-546.

26 V. Derbyshire, N. D. F. Grindley and C. M. Joyce, *Embo. J.*, 1991, **10**, 17-24.

27 S.-L. Chen, W. -H. Fang and F. Himo, *J. Phys. Chem. B*, 2007, **111**, 1253-1255.

28 J. Kim, P. C. Tsai, S. -L. Chen, F. Himo, S. C. Almo and F. M. Raushel, *Biochemistry*, 2008, **47**, 9497-9504.

29 S. D. Aubert, Y. Li and F. M. Raushel, *Biochemistry*, 2004, **43**, 5707-5715.

30 B. L. Martin and D. J. Graves, *J. Biol. Chem.*, 1986, **261**, 14545-14550.

31 B. L. Martin and D. J. Graves, *Biochim. Biophys. Acta.*, 1994, **1206**, 136-142.

32 M. D. Jackson and J. M. Denu, *Chem. Rev.*, 2001, **101**, 2313-2340.

33 R. -Z. Liao, J. -G. Yu and F. Himo, *J. Phys. Chem. B*, 2010, **114**, 2533-2540.

34 R. -Z. Liao, J. -G. Yu and F. Himo, *Inorg. Chem.*, 2010, **49**, 6883-6888.

35 R. -Z. Liao, F. Himo, J. -G. Yu and R. -Z. Liu, *Eur. J. Inorg. Chem.*, 2009, **2009**, 2967-2972.

36 A. D. Becke, *J. Chem. Phys.*, 1993, **98**, 1372-1377.

37 A. D. Becke, *J. Chem. Phys.*, 1993, **98**, 5648-5652.

38 C. Lee, W. Yang and R. G. Parr, *Phys. Rev. B.*, 1988, **37**, 785-789.

39 Jaguar, *version 7.6*, Schrodinger, LLC, New York, NY, 2009.

40 P. J. Hay and W. R. Wadt, *J. Chem. Phys.*, 1985, **82**, 299-310.

41 D. J. Tannor, B. Marten, R. Murphy, R. A. Friesner, D. Sitkoff, A. Nicholls, M. Ringnalda, W. A. Goddard III and B. Honig, *J. Am. Chem. Soc.*, 1994, **116**, 11875-11882.

42 B. Marten, K. Kim, C. Cortis, R. A. Friesner, R. B. Murphy, M. N. Ringnalda, D. Sitkoff and B. Honig, *J. Phys. Chem.*, 1996, **100**, 11775-11788.

43 M. R. Blomberg, T. Borowski, F. Himo, R. -Z. Liao and P. E. M. Siegbahn, *Chem. Rev.*, 2014**, 114**, 3601-3658.

44 F. Himo and P. E. M. Siegbahn, *Chem. Rev.*, 2003, **103**, 2421-2456.

45 P. E. M. Siegbahn, *Q. Rev. Biophys*., 2003, **36**, 91-145.

46 M. J. Frisch, G. W. Trucks, H. B. Schlegel, G. E. Scuseria, M. A. Robb, J. R. Cheeseman, J. A. Montgomery, Jr., T. Vreven, K. N. Kudin, J. C. Burant, J. M. Millam, S. S. Iyengar, J. Tomasi, V. Barone, B. Mennucci, M. Cossi, G. Scalmani, N. Rega, G. A. Petersson, H. Nakatsuji, M. Hada, M. Ehara, K. Toyota, R. Fukuda, J. Hasegawa, M. Ishida, T. Nakajima, Y. Honda, O. Kitao, H. Nakai, M. Klene, X. Li, J. E. Knox, H. P. Hratchian, J. B. Cross, V. Bakken, C. Adamo, J. Jaramillo, R. Gomperts, R. E. Stratmann, O. Yazyev, A. J. Austin, R. Cammi, C. Pomelli, J. W. Ochterski, P. Y. Ayala, K. Morokuma, G. A. Voth, P. Salvador, J. J. Dannenberg, V. G. Zakrzewski, S. Dapprich, A. D. Daniels, M. C. Strain, O. Farkas, D. K. Malick, A. D. Rabuck, K. Raghavachari, J. B. Foresman, J. V. Ortiz, Q. Cui, A. G. Baboul, S. Clifford, J. Cioslowski, B. B. Stefanov, G. Liu, A. Liashenko, P. Piskorz, I. Komaromi, R. L. Martin, D. J. Fox, T. Keith, M. A. Al-Laham, C. Y. Peng, A. Nanayakkara, M. Challacombe, P. M. W. Gill, B. Johnson, W. Chen, M. W. Wong, C. Gonzalez and J. A. Pople, Gaussian 03, Revision E.01, Gaussian, Inc., Wallingford CT, 2004.

47 R. -Z. Liao and W. Thiel, *J. Phys. Chem. B*, 2013, **117**, 3954-3961.

48 S. -L. Chen, W. -H. Fang and F. Himo, *Theor. Chem. Acc.*, 2008, **120**, 515-522.

49 S. Grimme, *J. Comput. Chem*., 2004, **25**, 1463–1473.

50 S. Grimme, *J. Comput. Chem.*, 2006, **27**, 1787–1799.

51 S. Grimme, J. Antony, S. Ehrlich and H. Krieg, *J. Chem. Phys.*, 2010**, 132**, 154104.

52 L. Goerigk and S. Grimme, *Phys. Chem. Chem. Phys.*, 2011**, 13**, 6670-6688.

53 H. -M. Zhang and S. -L. Chen, *J. Chem. Theory Comput.*, 2015, **11**, 2525-2535.

54 P. E. M. Siegbahn, *J. Comput. Chem.*, 2001**, 22**, 1634-1645.

55 R. A. M. O'Ferrall, *J. Chem. SOC. B*, 1970, 274-277.

56 W. P. Jencks, *Chem. Rev.*, 1985, **85**, 511-527.

57 K. M. Holtz, I. E. Catrina, A. C. Hengge and E. R. Kantrowitz, *Biochemistry*, 2000, **39***,* 9451-9458.

58 C. J. Jackson, J. L. Foo, H. K. Kim, P. D. Carr, J. -W. Liu, G. Salem and D. L. Ollis, *J. Mol. Biol.*, 2008 **375***,* 1189–1196.

Table of contents entry

A novel μ$_3$-oxo stabilized by three cations is demonstrated to be a sufficient nucleophile in the hydrolysis of phosphate esters.

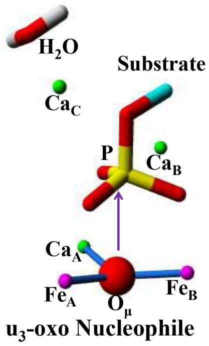
H_2O
Substrate
Ca_C
P
Ca_B
Ca_A
Fe_A
Fe_B
O_μ
u_3-oxo Nucleophile